# Absorbing phase transition in conserved lattice gas model on fractal lattices

Sang B. Lee* and Yun Nam Kim
*Department of Physics, Kyungpook National University, Taegu 702-701 Korea*
(Received 31 March 2007; published 27 September 2007)

We study the continuous phase transition of the conserved lattice gas (CLG) model from an active phase into an absorbing phase on two fractal lattices, i.e., on a checkerboard fractal and on a Sierpinski gasket. In the CLG model, a particle is assumed to be active if any of the neighboring sites are occupied by a particle and inactive if all neighboring sites are empty. We estimate critical exponents $\theta$, $\beta$, $\nu_{\parallel}$, and $\nu_{\perp}$, characterizing, respectively, the density of active particles in time, the order parameter, the temporal and spatial correlation lengths near the critical point, and the results are confirmed by off-critical scaling and finite size scaling. The order parameter exponent $\beta$ on a checkerboard fractal appears to lie between the one-dimensional (1D) value and two-dimensional (2D) value of the CLG model, while that on a Sierpinski gasket lies between the 1D and 2D values of the conserved threshold transfer process. Such a difference is manifested based on the intrinsic properties of the underlying fractal lattices.

DOI: 10.1103/PhysRevE.76.031137 PACS number(s): 05.70.Ln, 05.50.+q, 64.60.Ht

## I. INTRODUCTION

The nonequilibrium phase transition from a fluctuating phase into one or more absorbing states has attracted great interest in recent years [1–4]. The most prominent and well-known universality class is the directed percolation (DP) class [5]. A typical example of a model which belongs to the DP class is the contact process (CP) with a reaction-diffusion scheme $A \to 2A$ and $A \to 0$, in which each particle either creates an offspring with a rate $\lambda$ or annihilates with a rate $\mu$. Many other models with quite different evolution rules were also found to belong to the DP universality class, suggesting the robustness of the DP class [1–4]. According to the conjecture proposed by Janssen and Grassberger, any continuous phase transition from a fluctuating phase into a single absorbing state in a homogeneous, one-component system with short-range interactions should belong to the DP class, provided that there are no additional conservation laws, quenched randomness, or unconventional symmetries [6,7]. However, various systems with many absorbing states have also been found to belong to the DP class [8–10]. An example of such a model is the pair contact process (PCP), in which pairs of particles either annihilate with probability $p$ or create a new particle on the randomly chosen empty nearest-neighbor site ($2A \to 0$, $2A \to 3A$). Since each particle is not allowed to diffuse, all isolated particles are inactive and, therefore, systems with all particles isolated are in the absorbing states. Despite the existence of many absorbing states, the PCP model has been known to belong to the DP class. (Note that exponents consistent with the DP class were obtained only when the dynamics proceed from the system-generated initial configuration [8].)

The other widely known universality class is the parity-conserving (PC) class, observed with additional symmetries. The PC class is most likely represented by branching annihilating random walks with an even number of offsprings (BARW-$n$), in which each particle either jumps to a nearest-neighbor site with a probability $p$ or produces $n$ offsprings on $n$ nearest-neighbor sites [$A \to (n+1)A$] with a probability $1-p$ [11–14]. When a particle jumps to an already occupied site and when an offspring is created on such a site, both the incoming particle and the occupying particle annihilate each other ($AA \to 0$), leaving the site empty. When $n$ is even, the number of particles is conserved modulo 2, and this conservation law is believed to be responsible for the non-DP behavior. When $n$ is odd, on the other hand, since the last remaining particle may produce an odd number of offspring and pairs of particles are annihilated, the absorbing phase is a single vacuum state. The BARW-$n$ model with odd $n$, thus, satisfies the DP hypothesis and belongs to the DP class.

Another, yet controversial, universality class is the pair contact process with diffusion (PCPD) class. The term PCPD originated from the PCPD model, which is a variant of the PCP model, obtained by allowing diffusion of each particle to the neighboring empty site. The PCPD model was originally reported to belong to a new universality class [15–17]; however, its critical behavior is still in controversy mainly due to a slow convergence to the asymptotic limit [18].

Recently Rossi *et al.* proposed a lattice model with a conserved field, called the conserved lattice gas (CLG) model [19]. In the CLG model, a particle is defined as active if it has at least one particle in the nearest-neighbor sites. If a particle is surrounded by empty sites, it is considered to be inactive. The dynamics proceed by only a repulsive interaction, i.e., each active particle tends to hop to one of the empty nearest-neighbor sites. Thus, there is no particle creation and annihilation, no external field which converts an inactive particle to an active one, and no self-diffusion. Rossi *et al.* found from Monte Carlo simulations in two dimensions that the measured critical exponents of the CLG model coincide with those of the conserved threshold transfer processes (CTTP) [9] and the stochastic sandpile models [20], indicating that all these models belong to the same universality class.

More recently Lübeck carried out extensive simulations for the CLG model in two, three, four, and five dimensions and showed that the critical exponents in four and five di-

*Corresponding author; sblee@knu.ac.kr

 

mensions are identical, implying that the upper critical dimension of the CLG model is four [21]. He also carried out simulations for both the CLG model and the CTTP model with an external field which converts an inactive particle to an active one [22–24]. The CTTP model is a modification of the threshold transfer process [9]. In this model, each lattice site may be empty, occupied by one particle, or occupied by two particles. Empty and singly occupied sites are considered inactive, whereas doubly occupied sites are considered active. In the latter case, one tries to transfer both particles on a given active site to randomly selected nearest-neighbor sites. If all neighboring sites are occupied by two particles, the transfer stops. Lübeck found that the exponents estimated for the CLG model were indeed close to those of the CTTP model in two and three dimensions.

In one dimension, however, it is known that a universality split occurs due to the distinct features of the CLG model from the CTTP model. The order parameter exponent $\beta$ was found to decrease from 1.0 to 0.64 as the dimensionality $d$ decreased from 4 to 2 for both CLG and CTTP models, and it jumped to 1.0 at $d=1$ for the CLG model [25], whereas it decreased monotonically down to 0.382 at $d=1$ for the CTTP model. The CLG model in one dimension has two symmetric absorbing phases at the critical density of $\rho_c=0.5$, i.e., 010 101$\cdots$ and 101 010$\cdots$, while in higher dimensions, many absorbing states exist. In addition, the dimensional reduction yields the particle hopping deterministic; i.e., each active particle in the CLG model has an occupied nearest-neighbor site in one of two directions and an empty site in an opposite direction. Therefore, the site to which an active particle jumps is determined by a local conformation, rather than by random selection. In the CTTP model, on the other hand, since each active site may have one or two neighboring inactive sites depending on the conformations, the sites to transfer the particles may be determined stochastically. The symmetric absorbing states at the critical density and the deterministic jump are the characteristic features of the CLG model which are distinct from the CTTP model, and it has been conjectured that at least one of these two features might be responsible for such a split of the universality class. We are interested in which of the features is the major source of the universality split. Recent work by Park *et al.* demonstrated that a conserved lattice model of two species of particles having two symmetric absorbing states indeed yielded critical exponents different from the known models [25].

In this paper, we investigate the continuous phase transition of the CLG model on two selected fractal lattices with a dimensionality between 1 and 2. We are particularly interested in how the exponent $\beta$ varies on two selected fractal lattices, i.e., on a checkerboard fractal and on a Sierpinski gasket [26,27]. On both fractal lattices, the CLG model no longer has symmetric absorbing states at critical density and jumps of active particles are not fully deterministic. However, jumps on a checkerboard fractal appear to be more likely deterministic due to the intrinsic properties of the no-loop structure and less number of nearest-neighbor sites. On the other hand, a Sierpinski gasket has the coordination number four, i.e., all sites have four nearest-neighbor sites and, accordingly, jumps of active particles are stochastic. Therefore, if the symmetric absorbing states at criticality are responsible for the universality split, the value of $\beta$ of the CLG model on both lattices will follow the trend of the CTTP model (i.e., both models will belong to the same universality class). On the other hand, if the results for the two fractal lattices are distinctly different, the deterministic feature of the CLG model might be the major cause of such a universality split. Therefore, we expect that our work on the two fractal lattices will shed light on the universality split.

The absorbing phase transition (APT) may be influenced by the intrinsic properties, such as ramification, connectivity, and lacunarity of the fractal lattice as well as by the fractional dimensionality. Earlier work by Gefen *et al.* on equilibrium systems demonstrated that the critical behavior depends on the details of the construction of the fractal [28]. In order to clarify such possibilities on the APT, we performed preliminary simulations for the CP model on two distinctly different fractal lattices, a checkerboard fractal and a Sierpinski *carpet*, the former of which is a finitely ramified fractal and the other is an infinitely ramified fractal. ("Finitely ramified" implies that any part of the fractal may be isolated from the rest by cutting out a finite number of bonds.) Our preliminary results, compared with the interpolated results of the Monte Carlo measurements on regular lattices, indicated that the critical exponents of the APT were influenced only by the lattice dimensionality for a checkerboard fractal, while for a Sierpinski carpet, the intrinsic properties appeared to have a nontrivial effect [29]. Assuming that similar results would also be observed for the CLG model, we expect that the intrinsic properties other than those discussed in the preceding paragraph would not alter the critical behavior for the selected finitely ramified fractal lattices.

The paper is organized as follows. In Sec. II, the generation method of the fractal lattices and Monte Carlo method for the CLG model will be described. In Sec. III, results will be presented with appropriate discussions and, finally in Sec. IV, the summary and the concluding remarks will be presented.

## II. MODELS AND SIMULATION METHODS

The simulation method consists of two steps. First, one must generate a fractal lattice of the desired size and, second, one must carry out the dynamics of the CLG model.

The underlying fractal lattices we selected are the checkerboard fractal and the Sierpinski gasket both of which are embedded in a two-dimensional space. The checkerboard fractal is generated by the following steps. In the first generation, a single square is divided into nine identical but smaller squares and the alternately placed four off-diagonal squares are eliminated. In the second and higher generations, each remaining square is again divided and the alternate four squares are eliminated. The same fractal lattice may be obtained alternatively by iterative growing processes [27]. After the $k$th generation is completed, the number of squares is $N(L)=5^k$ and the length of the edge of the system is $L=3^k a$, where $a$ is the lattice constant and may be set $a=1$. Assuming that each square consists of a unit mass, the fractal dimension is obtained as $d_F=\ln N(L)/\ln L=\ln 5/\ln 3$. In the constructed fractal, the lattice site is assumed to be at the

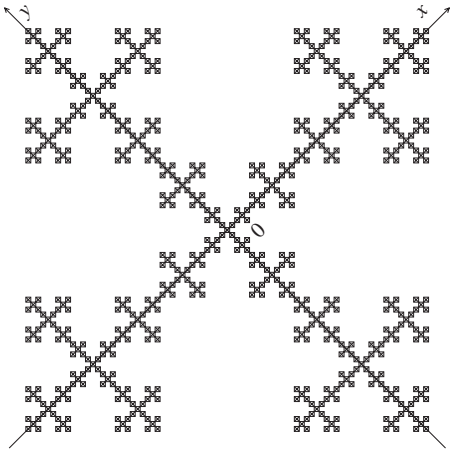


FIG. 1. The sample checkerboard fractal lattice generated up to four generations. The coordinates are set along the two diagonal directions, and any two sites on the nearest-neighbor squares along the diagonal directions are assumed to be connected.

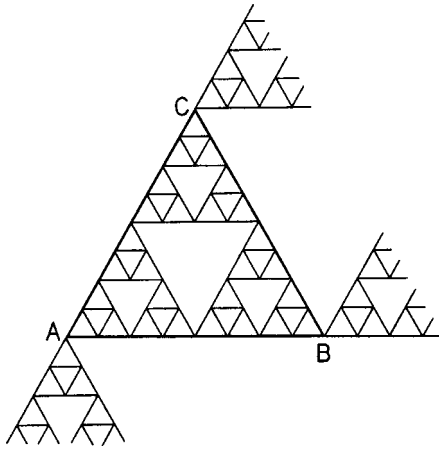


FIG. 2. The original cell *ABC* of the Sierpinski gasket and the parts of its replicated cells placed at the three corners. For the periodicity conditions, see text.

center of each remaining square. Since all the nearest-neighbor squares of the remaining square are eliminated, all lattice sites are surrounded by empty spaces, and the nearest-neighbor undeleted squares are located along the diagonal directions. Therefore, assuming the bonds between two nearest-neighbor sites along the diagonal directions, one can construct the connected fractal lattice. The sample fractal lattice generated up to four generations is shown in Fig. 1.

The Sierpinski gasket can be generated similarly. In the first generation, a single triangle is divided into four smaller triangles by connecting the three midpoints of the edges of the triangle and the inverted triangle at the center is eliminated. In the second and higher generations, each remaining triangle is again divided and the inverted one is eliminated. The lattice sites are assumed at the corners of the triangles. The total number of lattice sites in the Sierpinski gasket generated up to the $k$th order is $N(L)=6+\frac{3^{k+1}-9}{2}$ and the length of the edge of the system is $L=2^k$. The fractal dimension is, thus, given as $d_F=\ln N(L)/\ln L \to \ln 3/\ln 2$ as $k\to\infty$. It should be noted that the fractal dimension calculated with the mass of the sites is identical to that calculated with the mass of the unit triangles only when the fractal is infinitely large.

The dynamics of the CLG model proceed as follows. Initially $\rho N$ particles are distributed on the randomly selected sites of the given fractal lattice, where $N$ is the total number of sites on the underlying fractal lattice. In each time step, an active particle is selected from the list of active particles and it attempts to jump to one of the nearest-neighbor sites. If the selected site is already filled by a particle, the current trial is discarded and, otherwise, a jump is made. In each trial, the evolution time is increased by $1/N_a$, $N_a$ being the number of active particles. When an active particle at one of the corner sites is selected, a particle may either jump out of the system or be reflected by the boundary. Therefore, it is necessary to setup boundary conditions.

The number of boundary sites of the checkerboard fractal is four, while it is three for the Sierpinski gasket. For a checkerboard fractal, considering that the current cell is a part of the larger cell of a higher order generation, the four replicated cells can be assumed to be at the four corners of the given cell. Then, when a particle exits along the $+x$ $(+y)$ axis, the particle is assumed to reenter the system through the $-x$ $(-y)$ axis at the opposite corner, or vice versa. For a Sierpinski gasket, the replicated cells may be assumed analogously, but the same periodicity may not be warranted. The three replicated cells may be assumed to be at the three corners, as shown in Fig. 2. When a particle exits through point $B$ or $C$, it can be assumed to reenter through point $A$ along the same direction as it exited. However, the reverse does not hold. For example, assuming that a particle exits through point $B$, it reenters the cell through point $A$. When the same particle attempts to reexit through point $A$, it should reenter the cell through point $B$ since it entered point $A$ via point $B$. However, the periodicity of the cell allows the particle which exited through point $A$ to reenter through point $C$. Therefore, the periodicity along the horizontal direction fails. Such a failure of the periodicity may be resolved by coloring only the particles which exited the cell through point $B$ and reentered through point $A$. When colored particles exit the cell through point $A$, they are restricted to reentering the cell only through point $B$. In order to speed up the calculations, we avoid such a tedious procedure and apply the reflective boundaries, assuming that particles at the three corners of the cell always reflect from the boundary. We find that a different boundary condition influences only the nonuniversal critical point, leaving the critical exponents unchanged.

## III. RESULTS AND DISCUSSIONS

In most of our simulations, the checkerboard fractal is generated up to the seventh order with 78 125 lattice sites and the Sierpinski gasket up to the eleventh order with 265 722 sites. We also generate one higher order for both cases whenever the selected size is determined to be insufficient. The CLG model is simulated up to $10^7$ time steps.

Since the dynamics proceed by active particles, the density of the active particles, $\rho_a$, is the main interesting quan-

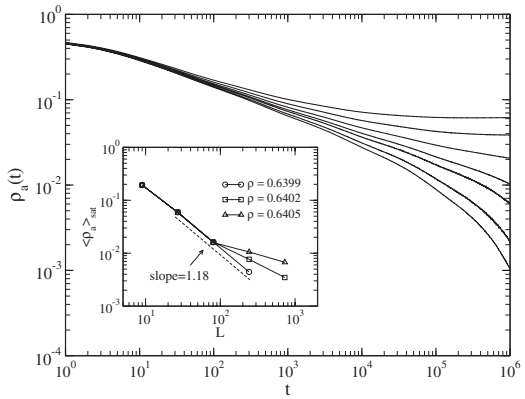


FIG. 3. The density of the active particles $\langle \rho_a \rangle$ against the evolution time for various values of the particle density $\rho$, i.e., from bottom to top, $\rho=0.635$, 0.6365, 0.6385, 0.6399, 0.642, 0.645, and 0.649, for the CLG model on a checkerboard fractal. The inset is the saturation density for three selected values of the particle density. The power law is observed for $\rho=0.6399$.

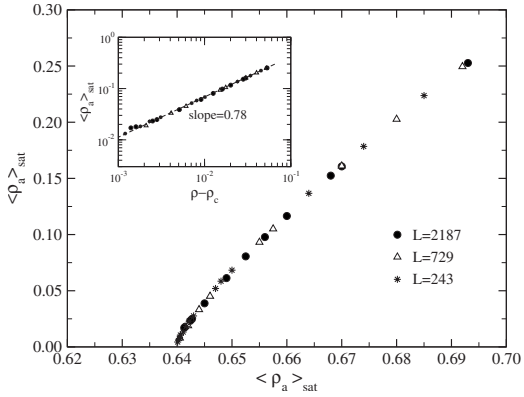


FIG. 4. The stationary density of the active particles $\langle \rho_a \rangle_{\text{sat}}$ plotted against the particle density $\rho$ for the CLG model on a checkerboard fractal of the size $L=3^5$, $3^6$, and $3^7$. The stationary density converges to 0 at the particle density $\rho \simeq 0.64$. The inset is the double logarithmic plot.

tity. Starting with the particles of density $\rho$ distributed randomly, $\rho_a$ decreases, as the dynamics proceed, from its initial value by the hopping of the active particles. If $\rho$ is sufficiently small, $\rho_a$ decreases rapidly and vanishes. On the other hand, if $\rho$ is large, $\rho_a$ never vanishes and it approaches a steady-state value as $t \to \infty$. The system, thus, undergoes a phase transition from an inactive phase to an active phase at the critical density $\rho_c$, at which $\rho_a$ decreases algebraically as $\rho_a \sim t^{-\theta}$. Thus, the ordering of the system is determined by the saturated, steady-state density $\langle \rho_a \rangle_{\text{sat}}$, which is considered to be an order parameter of the system.

The data of $\rho_a$ in general exhibits large fluctuations, particularly at $\rho_c$, due to the diverging range of interactions at criticality. In order to reduce such fluctuations, we take geometrical averages (arithmetic averages in a double logarithmic scale) of data within an interval of $\Delta(\ln t)=0.001$ and plot the results on the average time in the same interval. We find that this method not only reduces fluctuations but allows us to save disk space.

### A. The CLG model on a checkerboard fractal

Figure 3 shows the mean active particle density $\langle \rho_a \rangle$ against the evolution time. For $\rho > 0.642$, $\langle \rho_a \rangle$ appears to converge and, for $\rho < 0.639$, it decreases more rapidly than a power law. Therefore, the critical density is between 0.639 and 0.642. The determination of $\rho_c$ is not simple because of a finite size effect. Rossi *et al.* pointed out that, for a finite size system on a regular lattice in two dimensions, the active particle density followed a power-law behavior in the early-time stage and decreased faster than a power law and eventually saturated as $t \to \infty$. We find that the CLG model on a checkerboard fractal exhibits a similar behavior and the determination of the critical density is extremely difficult due to the finite size effect. Despite such a difficulty, we determine $\rho_c=0.6399$ for a checkerboard fractal. The critical density is determined by two different ways. First, the steady-state value, i.e., the order parameter, vanishes at $\rho_c$ as $\langle \rho_a \rangle_{\text{sat}} \sim (\rho-\rho_c)^{\beta}$. From the plot in Fig. 3, the critical density appears to be slightly smaller than but close to 0.64, i.e., $\rho_c=0.6399$. Second, for a finite size system, the order parameter is in practice a function of two variables, i.e., the size of the system $L$ and the spatial correlation length $\xi_{\perp}$, the latter of which is characterized by the distance from the criticality $\rho-\rho_c$ via $\xi_{\perp} \sim |\rho-\rho_c|^{-\nu_{\perp}}$. Using the basic scaling concepts [30], the order parameter can be written as $\langle \rho_a \rangle_{\text{sat}} = L^{-\beta/\nu_{\perp}} f(L|\rho-\rho_c|^{\nu_{\perp}})$. Therefore, at $\rho=\rho_c$, the order parameter is expected to show a power law $\langle \rho_a \rangle_{\text{sat}} \sim L^{-\beta/\nu_{\perp}}$. On the other hand, if the density is away from the criticality, the order parameter is no longer a function of a single variable, nor shows a power-law behavior in $L$. We calculate the order parameter for $L=3^3$, $3^4$, $3^5$, and $3^6$ and find that the plot of $\langle \rho_a \rangle_{\text{sat}}$ yields a power law at $\rho_c=0.6399$ with the power $\beta/\nu_{\perp}=1.182(5)$, as shown in the inset of Fig. 3. (Note that the number in parentheses denotes the uncertainty of the last digit.) With the estimate of $\rho_c$, we obtain $\theta=0.287(3)$ from the regression fit of $\langle \rho_a \rangle$ in the large $t$ region before the finite size effect sets in. The order parameter exponent $\beta$ is also obtained as $\beta=0.780(2)$ from the power-law fit of $\langle \rho_a \rangle_{\text{sat}}$ versus $\rho-\rho_c$, as in the inset of Fig. 4. The spatial correlation-length exponent is, thus, $\nu_{\perp}=0.66(5)$. A careful analysis of the data in the inset shows that the data for $\rho$ close to $\rho_c$ deviate from the regression fit. We believe it to be due to the finite size effect. It should be noted, however, that assuming the critical density as a parameter and attempting to fit the whole region of the data, the best fit would be obtained for $\rho_c \simeq 0.6395$, which is smaller than the critical density obtained above. However, for this value, one would obtain critical exponents also different from those obtained above. We find that with the exponents obtained by this method the off-critical scaling does not hold.

The estimated critical exponents can be confirmed by the off-critical scaling and finite size scaling. Consider $\langle \rho_a \rangle$ at the particle density $\rho$ and at the evolution time $t$. Then, $\langle \rho_a \rangle$ near the critical point is a function of $t$ and the temporal correlation function $\xi_{\parallel}$, the latter of which is characterized by the distance from the criticality via $\xi_{\parallel} \sim |\rho-\rho_c|^{-\nu_{\parallel}}$. The scal-

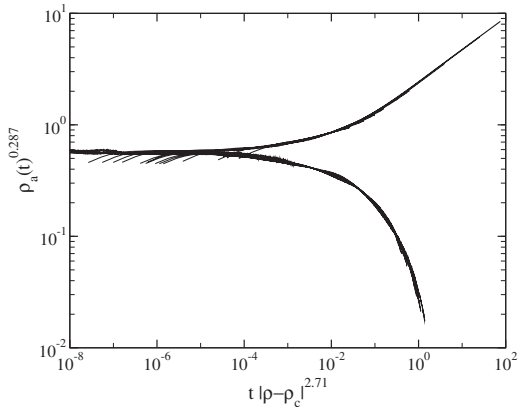


FIG. 5. The off-critical scaling function of the active particle density plotted against the scaled variable $x \equiv t|\rho-\rho_c|^{\nu_\parallel}$ with $\nu_\parallel = 2.71$, for the CLG model on a checkerboard fractal. Data for various values of the particle density collapse onto two separate curves, depending on whether the particle density is larger or small than the critical density.

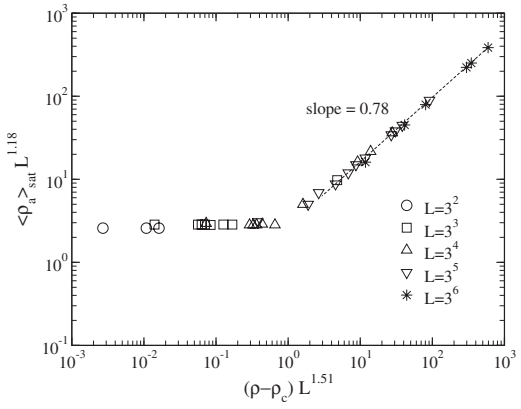


FIG. 6. The finite-size scaling function of the stationary density of active particles $\langle\rho\rangle_{\rm sat} L^{\beta/\nu_\perp}$ as a function of $|\rho-\rho_c|L^{1/\nu_\perp}$, for the CLG model on a checkerboard fractal. The scaling powers used are $\beta/\nu = 1.18$ and $1/\nu_\perp = 1.51$.

ing idea again allows us to write $\langle\rho_a\rangle$ as a function of a single variable, i.e., $\langle\rho_a\rangle = t^{-\theta} g(t|\rho-\rho_c|^{\nu_\parallel})$, $g(x)$ being the scaling function of the scaled variable $x \equiv t|\rho-\rho_c|^{\nu_\parallel}$. Considering $\langle\rho_a\rangle$ in the supercritical region in the $t\to\infty$ limit, it becomes the order parameter, yielding $\langle\rho_a\rangle_{\rm sat} \sim (\rho-\rho_c)^{\nu_\parallel\theta} \sim (\rho-\rho_c)^{\beta}$. Thus, the scaling relation $\beta = \theta\nu_\parallel$ is obtained. Using our estimates of $\theta$ and $\beta$, we get $\nu_\parallel = 2.71$.

The off-critical scaling function $g(x)$ is plotted in Fig. 5 against the scaled variable $x \equiv t|\rho-\rho_c|^{\nu_\parallel}$. Data for various values of the particle density collapse onto two separate curves, one for $\rho > \rho_c$ (upper curve) and the other for $\rho < \rho_c$ (lower curve). The alternate thick and slim parts of the data which collapse for $\rho < \rho_c$ are due to the wiggling of the Monte Carlo data, caused presumably by the underlying lattice structure, as one can observe in Fig. 3. We examine the same scaling with $\rho_c = 0.6395$ and the exponents estimated using this value as a critical density; however, we find that data do not collapse. We, thus, confirm that our estimates for $\rho_c$, $\beta$, and $\theta$ are valid.

The finite size scaling is also tested using the data for smaller systems. Since our system is fractal, we pick the linear size of the system as a multiple of 3, i.e., $L = 3^4$, $3^5$, $3^6$, and $3^7$, and the steady-state density is calculated for various values of $\rho$ above the critical point. Figure 6 shows the scaled density $\langle\rho_a\rangle_{\rm sat} L^{\beta/\nu_\perp}$ against the scaled variable $|\rho-\rho_c|L^{1/\nu_\perp}$. Data for various sized systems and various densities near criticality indeed scale with our estimates, implying that the values of $\beta$ and $\nu_\perp$ are correct. The asymptotic slope for the data beyond the criticality is 0.78, which is identical to the value of $\beta$, as expected.

### B. CLG model on a Sierpinski gasket

For the CLG model on a Sierpinski gasket, we employ the reflective boundary condition by the reason we described in Sec. II. The reflective boundary condition in general yields the finite size effect more significantly than the periodic boundary condition. However, we believe that the two boundary conditions yield eventually the same critical behavior, although the nonuniversal critical density might be different.

We realize that the determination of the critical density for the CLG model on a Sierpinski gasket is more difficult than for the same model on a checkerboard fractal, apparently due to the finite size effect. As a test, we assume the critical density as such that yields $\langle\rho_a\rangle$ a power-law behavior in the long time limit, up to $10^7$ time steps. We find that $\langle\rho_a\rangle$ exhibits the best linear behavior on a double logarithmic scale at $\rho = 0.318\,395$. The power-law behavior is observed only for $t > 10^5$ with the power of $\theta = 0.213$ and the order parameter exponent is estimated as $\beta = 0.535$. However, we find that with these values neither the finite size scaling nor the off-critical scaling hold. Failure of the scalings is attributed to the incorrect exponents by the finite size effect.

The finite size effect for the CLG model on a Sierpinski gasket appears to influence $\langle\rho_a\rangle$ in such a way as to decay rapidly, rather than decrease and then saturate. This leads to the finite size scaling different from that on a checkerboard fractal, as we will see later. Thus, for a finite system, the active particle density decays in the large $t$ region even at the critical density. Because of this decreasing behavior, the power-law behavior may be observed at the density greater than the "true" critical density, at which the decaying behavior of $\rho_a$ due to the finite-size effect is canceled by a saturation in the supercritical region. As a consequence, the critical density cannot be determined correctly from the power-law behavior in the large $t$ region.

In order to determine the critical density, we assume the density which yields the widest region of the power-law behavior as the critical density. We find that $\langle\rho_a\rangle$ exhibits perfect power-law behavior in the region of $10 \leqslant t \leqslant 10^5$ and then decays rapidly for $\rho = 0.317\,90$. Data for a slightly larger value of $\rho$, e.g., $\rho = 0.317\,905$, appear to yield a slight bump just before the decay sets in (not shown). We believe that such a bump is a precursor of saturation, while the decay is the finite size effect, indicating that this value of $\rho$ is already above the critical point. We, therefore, determine

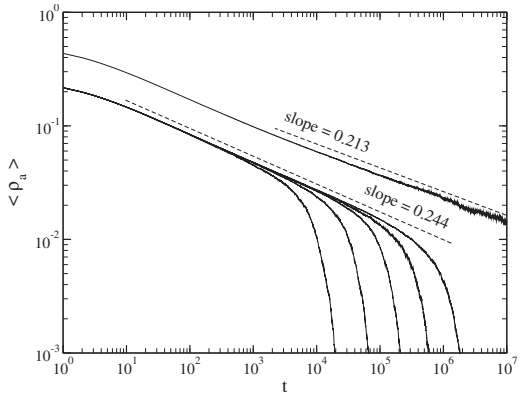


FIG. 7. The density of the active particles $\langle \rho_a \rangle$ against the evolution time for $\rho=0.318\,39$ and $L=2^{11}$ (upper plot) and for $\rho=0.317\,90$ and various size systems (lower sets), i.e., from left to right, $L=2^8$, $2^9$, $2^{10}$, $2^{11}$, and $2^{12}$, for the CLG model on a Sierpinski gasket. The upper data are those multiplied by 3 on the original data to avoid overlap.

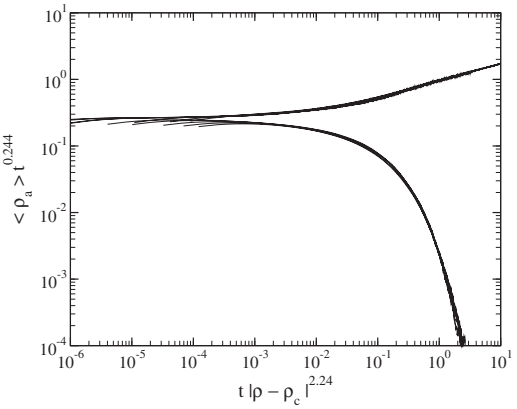


FIG. 8. The scaled density of the active particles $\langle \rho_a \rangle t^\theta$ against the scaled time of evolution $t|\rho-\rho_c|^{\nu_\parallel}$, for the CLG model on a Sierpinski gasket. Data are for $0.30 \leqslant \rho \leqslant 0.315$ below the critical point of $\rho_c=0.317\,90$ and for $0.319 \leqslant \rho \leqslant 0.3335$ above the critical point.

$\rho_c=0.317\,90(5)$. We believe that our estimate is accurate based on the fact that exponents estimated using this value yield the best data collapsing in both the off-critical scaling and the finite size scaling, as we will see later.

Figure 7 shows $\langle \rho_a \rangle$ for various sized systems at $\rho_c$ plotted against the evolution time. The upper data are for $\rho=0.318\,395$ which yields the power-law behavior in the larger $t$ limit. (Note that the plot is shifted upward to avoid overlapping with the lower plots.) If we estimate the critical index from the power-law behavior in the large $t$ region, we could get $\theta=0.213$, $\beta=0.535$, and $\nu_\parallel=2.51$; however, with these values, the off-critical scaling does not hold. The lower plots in Fig. 7 are the data for $\rho_c=0.317\,90$ for various sized systems, i.e., for, from left to right, $L=2^8$, $2^9$, $2^{10}$, $2^{11}$, and $2^{12}$. The power-law region becomes wider, up to four decades, as expected from that the finite size effect decreases as the size of the system increases, and the power-law fit yields $\theta=0.244$ as shown by the dashed line in the plot. The steady-state density is calculated for various values of $\rho$ above $\rho_c$ and the order parameter exponent is estimated as $\beta=0.547(5)$. The exponent characterizing the temporal correlation length is thus $\nu_\parallel \simeq 2.24$.

In order to verify our estimates, we carry out the off-critical scaling. Shown in Fig. 8 are the data of the scaled densities of the active particles, $\langle \rho_a \rangle t^\theta$, plotted against the scaled variable $t|\rho-\rho_c|^{\nu_\parallel}$. Data for $0.30 \leqslant \rho \leqslant 0.315$ below $\rho_c$ and for $0.319 \leqslant \rho \leqslant 0.3335$ above $\rho_c$ fall on the same curve in each case. We, therefore, believe from this scaling that our determination of $\rho_c$ is correct and so are the critical exponents.

The exponent characterizing the spatial correlation length cannot be determined in this case by using the same method as the plot in the inset in Fig. 3 because $\langle \rho_a \rangle$ does not saturate at $\rho_c$ for a finite size system, unlike the case of the checkerboard fractal. We instead consider the time dependence of $\langle \rho_a \rangle$. Then, $\langle \rho_a \rangle$ is a function of two variables, i.e., $\langle \rho_a \rangle = f(t,L)$. From the scaling hypothesis, one can readily get the scaling relation $\langle \rho_a \rangle = t^{-\theta} f(t/L^z)$, where $z=\nu_\parallel/\nu_\perp$ is the dynamic exponent. We have tested the scaling function $f(x) = \langle \rho_a \rangle t^\theta$ plotting against the scaled variable $x \equiv t/L^z$, assuming the scaling exponent $z$ as a parameter. We find that the best collapsing of data is observed for $z=1.69(3)$, as shown in Fig. 9. From the scaling relation $z=\nu_\parallel/\nu_\perp$, we obtain $\nu_\perp=1.325(5)$.

## IV. SUMMARY AND CONCLUDING REMARKS

We have studied APT in the CLG model on a checkerboard fractal and on a Sierpinski gasket both of which are embedded in two dimensions. We have estimated the critical exponents $\theta$, $\beta$, $\nu_\perp$, and $\nu_\parallel$, which characterize, respectively, the density of the active particles in time, the order parameter, and the spatial and temporal correlations against the distance from the critical point. Results were confirmed by off-critical scaling and finite size scaling. The estimates are compared in Table I with the known values on regular lattices.

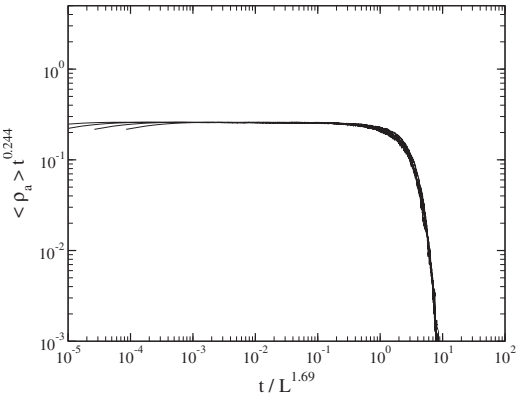


FIG. 9. The scaled densities of the active particles $\langle \rho_a \rangle t^\theta$ against the scaled time $t/L^z$ for various size systems, i.e., for $L=2^8$, $2^9$, $2^{10}$, and $2^{11}$, for the CLG model on a Sierpinski gasket. The critical indices used are $\theta=0.244$ and $z=1.69$.

TABLE I. Critical exponents for the conserved lattice gas model on fractal lattices, in comparison with those on regular lattices.

| | $\theta$ | $\beta$ | $\nu_{\parallel}$ | $\nu_{\perp}$ |
|---|---|---|---|---|
| 1D[a] | 0.247 | 0.99 | 4.05 | 2.0 |
| Checkerboard[b] | 0.287(3) | 0.780(2) | 2.71 | 0.66(5) |
| Sierpinski gasket[c] | 0.244 | 0.547(5) | 2.24 | 1.325(5) |
| 2D[d] | 0.43(1) | 0.637(9) | 1.46(5) | 0.29(1) |
| 3D[d] | | 0.837(15) | | |
| 4D[e] | | 1.0 | | |
| 5D[d] | | 1.0 | | |

[a]Our results using sequential updates (not reported).
[b]$d_F = \ln 5/\ln 3 \simeq 1.465$.
[c]$d_F = \ln 3/\ln 2 \simeq 1.585$.
[d]References [19] and [20].
[e]Reference [20].

Focusing on the order parameter exponents, it appears that the result for a checkerboard fractal lies on the interpolation line of the CLG model for the dimensionality between 1 and 2, while that for a Sierpinski gasket lies on the line of the CTTP model. This suggests that the CLG model might exhibit a different critical behavior from the CTTP model on a checkerboard fractal, whereas on a Sierpinski gasket two models might belong to the same universality class. As we pointed out in Sec. I, since the CLG model does not have symmetric absorbing states on both lattices, it appears clear that the symmetry of the absorbing states alone is not the primary cause of the universality split, but rather the determinism might be more responsible. We realize that exactly 40% of the lattice sites on a checkerboard fractal are on the dead ends, 40% are the sites with two nearest neighbors, and the remaining 20% are those with four neighbors. Considering that particles trapped on dead ends cannot jump and that active particles on sites with two neighbors jump deterministically, at least 60% of the jumps will be deterministic and less than 40% will be stochastic. Therefore, the deterministic hopping dominates the dynamics, and this appears to yield the dynamics of the CLG model different from those of the CTTP model. (Note that the transfer of particles from active sites in the CTTP model is stochastic unless dead ends are active sites.) The Sierpinski gasket, on the other hand, has a coordination number 4 with no dead ends and, therefore, the hopping of the active particles is most likely stochastic for both the CLG and the CTTP models.

From our results, we surmise that both the CLG model and the CTTP model on a Sierpinski gasket may belong to the same universality class, while on a checkerboard fractal, the two models might exhibit different behaviors. Examining whether or not this speculation is correct, by estimating full sets of exponents for both models on both fractal lattices, would be an interesting topic and such research is currently ongoing.

## ACKNOWLEDGMENT

This work was supported by the Korea Science and Engineering Foundation Grant No. R01-2004-000-10148-0. The authors are grateful for the support.

[1] J. Marro and R. Dickman, *Nonequilibrium Phase Transitions in Lattice Models* (Cambridge University Press, Cambridge, 1999).
[2] D. Ben-Avraham and S. Havlin, *Diffusion and Reaction in Fractals and Disordered Systems* (Cambridge University Press, Cambridge, 2000).
[3] H. Hinrichsen, Adv. Phys. **49**, 815 (2000).
[4] G. Ódor, Rev. Mod. Phys. **76**, 663 (2004).
[5] J. L. Cardy and R. L. Sugar, J. Phys. A **13**, L423 (1980).
[6] H. K. Janssen, Z. Phys. B: Condens. Matter **42**, 151 (1981).
[7] P. Grassberger, Z. Phys. B: Condens. Matter **47**, 365 (1982).
[8] I. Jensen and R. Dickman, Phys. Rev. E **48**, 1710 (1993).
[9] J. F. F. Mendes, R. Dickman, M. Henkel, and M. C. Marques, J. Phys. A **27**, 3019 (1994).
[10] M. A. Munoz, G. Grinstein, R. Dickman, and R. Livi, Phys. Rev. Lett. **76**, 451 (1996).
[11] H. Takayasu and A. Y. Tretyakov, Phys. Rev. Lett. **68**, 3060 (1992).
[12] I. Jensen, Phys. Rev. E **50**, 3623 (1994).
[13] S. Kwon and H. Park, Phys. Rev. E **52**, 5955 (1995).
[14] J. Cardy and U. C. Tauber, Phys. Rev. Lett. **77**, 4780 (1996).
[15] G. Odor, Phys. Rev. E **62**, R3027 (2000).
[16] H. Hinrichsen, Phys. Rev. E **63**, 036102 (2001).
[17] K. Park and I.-M. Kim, Phys. Rev. E **66**, 027106 (2002).
[18] M. Henkel and H. Hinrichsen, J. Phys. A **37**, R117 (2004).
[19] M. Rossi, R. Pastor-Satorras, and A. Vespignani, Phys. Rev. Lett. **85**, 1803 (2000).
[20] S. S. Manna, J. Phys. A **24**, L363 (1991); also see A. Vespignani, R. Dickman, M. A. Munoz, and S. Zapperi, Phys. Rev. Lett. **81**, 5676 (1998).
[21] S. Lübeck, Phys. Rev. E **64**, 016123 (2001).
[22] S. Lübeck, Phys. Rev. E **66**, 046114 (2002).
[23] S. Lübeck and A. Hucht, J. Phys. A **35**, 4853 (2002).
[24] S. Lübeck and P. C. Heger, Phys. Rev. E **68**, 056102 (2003).
[25] K. Park, S. Kang, and I.-M. Kim, Phys. Rev. E **71**, 066129 (2005).
[26] B. B. Mandelbrot, *The Fractal Geometry of Nature* (W. H. Freeman and Company, New York, 1983).
[27] T. Vicsek, *Fractal Growth Phenomena* (World Scientific, Singapore, 1992).
[28] Y. Gefen, B. B. Mandelbrot, and A. Aharony, Phys. Rev. Lett. **45**, 855 (1980); J. Phys. A **16**, 1267 (1983); **17**, 1277 (1984).
[29] S. B. Lee, Physica A (to be published).
[30] D. J. Amit, *Field Theory, the Renormalization Group, and Critical Phenomena* (World Scientific, Singapore, 1984).